

AD-A057 900

NAVAL POSTGRADUATE SCHOOL MONTEREY CALIF
SHIPBOARD STABILIZATION OF OPTICAL SYSTEMS. (U)
JUN 78 R L WILLIAMS

F/G 17/8

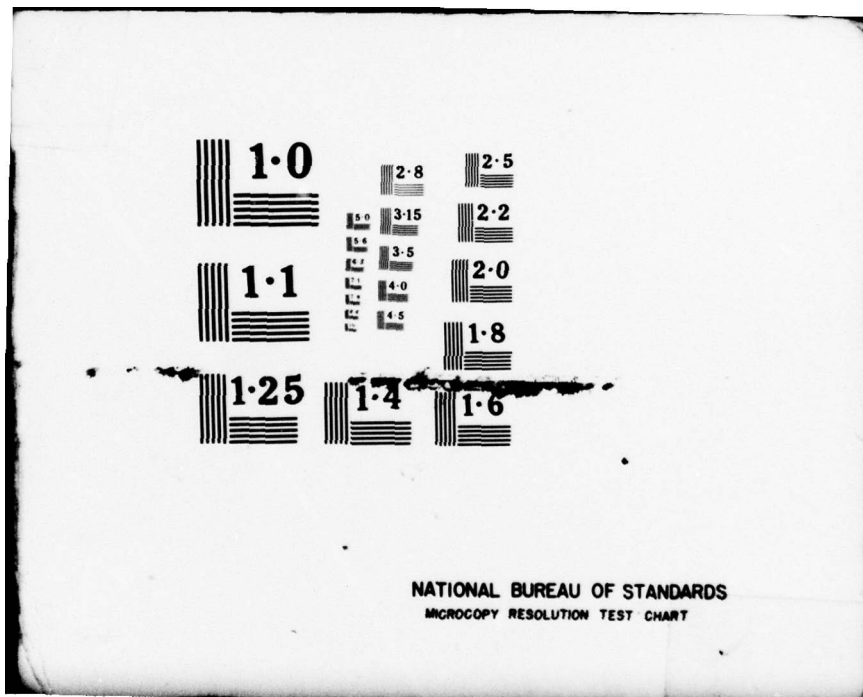
UNCLASSIFIED

NL

| OF |
ADA
057900



END
DATE
FILED
10 - 78
DDC



ADA 057900

AD No. 1
DDC FILE COPY

② LEVEL II
SC

NAVAL POSTGRADUATE SCHOOL
Monterey, California



DDC
REF ID: A
AUG 24 1978
REGIMENT B

THESIS

Shipboard Stabilization of Optical Systems

by

Robbie L. Williams

June 1978

Thesis Advisor:

E.C. Crittenden, Jr.

Approved for public release; distribution unlimited

78 08 23 04 4

SECURITY CLASSIFICATION OF THIS PAGE (When Data Entered)

REPORT DOCUMENTATION PAGE		READ INSTRUCTIONS BEFORE COMPLETING FORM
1. REPORT NUMBER	2. GOVT ACCESSION NO.	3. RECIPIENT'S CATALOG NUMBER
4. TITLE (and Subtitle)		5. TYPE OF REPORT & PERIOD COVERED Master's Thesis, June 1978
Shipboard Stabilization of Optical Systems.		6. PERFORMING ORG. REPORT NUMBER
7. AUTHOR(s)	8. CONTRACT OR GRANT NUMBER(s)	
Robbie L. Williams		
9. PERFORMING ORGANIZATION NAME AND ADDRESS Naval Postgraduate School Monterey CA 93940		10. PROGRAM ELEMENT, PROJECT, TASK AREA & WORK UNIT NUMBERS
11. CONTROLLING OFFICE NAME AND ADDRESS Naval Postgraduate School Monterey CA 93940		12. REPORT DATE June 1978
14. MONITORING AGENCY NAME & ADDRESS (if different from Controlling Office) Naval Postgraduate School Monterey CA 93940		13. NUMBER OF PAGES <i>1242p.</i>
		15. SECURITY CLASS. (of this report) Unclassified
		15a. DECLASSIFICATION/DOWNGRADING SCHEDULE
16. DISTRIBUTION STATEMENT (of this Report) Approved for public release; distribution unlimited.		
17. DISTRIBUTION STATEMENT (of the abstract entered in Block 20, if different from Report)		
18. SUPPLEMENTARY NOTES		
19. KEY WORDS (Continue on reverse side if necessary and identify by block number)		
20. ABSTRACT (Continue on reverse side if necessary and identify by block number) The control system for an existing shipboard gyrostabilized optic tracking platform was redesigned to achieve a longer tracking capability and improved tracking stability. The redesign increased the gain of the detector amplifier chain and improved the control system linearity. These modifications in conjunction with the addition of a mechanical viscous damper resulted in a three-fold increase in tracking range capability and significantly improved		

DD FORM 1 JAN 73 1473

EDITION OF 1 NOV 68 IS OBSOLETE
S/N 0102-014-66011

SECURITY CLASSIFICATION OF THIS PAGE (When Data Entered)

251 450 78 08 23 04 4 LB

tracking stability and reliability. The maximum tracking range of the system was estimated to exceed 6000 meters. The system tracking uncertainty is approximately +2.5 milliradians under "sea state" 5 and is less than this under normal conditions.

+ α -

REFERENCE NO.		
NAME	John Smith	
GRADE	1st Year	
CLASS	1995	
SECTION	101	
STUDY AVAILABILITY CODES		
Date: AVAIL and/or SPECIAL		
A		

Approved for public release; distribution unlimited

Shipboard Stabilization of Optical Systems

by

Robbie L. Williams
Lieutenant, United States Navy
B.S., University of Maryland, 1972

Submitted in partial fulfillment of the
requirements for the degree of

MASTER OF SCIENCE IN PHYSICS

from the

NAVAL POSTGRADUATE SCHOOL
June 1978

Author

R. Williams

Approved by:

E. L. Brustader, Jr.

Thesis Advisor

G. W. Rodekack

Second Reader

K. E. Walker

Chairman, Department of Physics and Chemistry

G. J. Haltiner

Dean of Science and Engineering

ABSTRACT

The control system for an existing shipboard gyro-stabilized optic tracking platform was redesigned to achieve a longer tracking range capability and improved tracking stability. The redesign increased the gain of the detector amplifier chain and improved the control system linearity. These modifications in conjunction with the addition of a mechanical viscous damper resulted in a three-fold increase in tracking range capability and significantly improved tracking stability and reliability. The maximum tracking range of the system was estimated to exceed 6000 meters. The system tracking uncertainty is approximately ± 2.5 milliradians under "sea state" 5 and is less than this under normal conditions.

TABLE OF CONTENTS

I.	INTRODUCTION	8
A.	BACKGROUND	8
B.	SYSTEM DESCRIPTION	9
II.	CONTROL SYSTEM THEORY	14
A.	STABILITY CRITERIA.....	14
B.	CLOSED LOOP FEEDBACK CONTROL.....	18
III.	DETAILED CONTROL SYSTEM DESCRIPTION.....	20
A.	DETECTOR.....	20
B.	DETECTOR PREAMPLIFIER.....	21
C.	VARIABLE GAIN AMPLIFIER.....	21
D.	RECTIFIER AND RIPPLE FILTER.....	23
E.	ANALOG COMPUTER.....	23
F.	MECHANICAL DAMPER.....	26
G.	POWER AMPLIFIER.....	26
H.	TWO-PHASE POWER DRIVER.....	27
I.	JOY STICK CONTROL.....	27
J.	GYRO CONTROL PANEL.....	27
IV.	TEST RESULTS.....	31
V.	CONCLUSIONS AND RECOMMENDATIONS.....	33
APPENDIX A:	Control Circuit Diagrams.....	34
APPENDIX B:	Control Circuit Adjustment Procedures.....	39
LIST OF REFERENCES.....		41
INITIAL DISTRIBUTION LIST.....		42

LIST OF FIGURES

1.	Diagram of Tracking Optics.....	10
2.	Control System Block Diagram.....	12
3.	Gyrostabilized Platform and Mounted Optics.....	13
4.	Diagram of Theoretical Dynamic Model.....	15
5.	Diagram of Control System Feedback Loops.....	19
6.	Tracking Telescope and Detector Head.....	22
7.	Gyro Control Panel.....	28
8.	Control System Electronics Cards.....	30
9.	Control Circuit Diagram, Section 1.....	35
10.	Control Circuit Diagram, Section 2.....	36
11.	Control Circuit Diagram, Section 3.....	37
12.	Two-Phase Power Driver Circuit Diagram.....	38

ACKNOWLEDGEMENT

The author would like to express his deep appreciation to Robert C. Smith for his invaluable effort towards the completion of this project and to Professor Eugene C. Crittenden for his continued guidance and assistance.

I. INTRODUCTION

A. BACKGROUND

Fog-aerosol concentrations have an important impact on optical transmission by causing extinction of optical beams. In addition, the absorption of optical radiation by fog-aerosol concentrations results in thermal blooming of high energy laser beams. This effect can have a dramatic impact on high energy laser beam propagation in a marine environment. Measurements of extinction in the marine boundary layer are required to establish a data base for future design of electro-optical systems for shipboard use. To evaluate the fog-aerosol extinction effects in the marine boundary layer, techniques were developed for ship to shore measurements. A gyrostabilized shipboard optical platform was needed and such a system was developed at the Naval Postgraduate School. A number of progressively improved systems were subsequently developed and utilized. Recent requirements for a longer tracking range capability and improved tracking stability prompted a control system redesign to achieve these requirements by increasing the gain of the detector amplifier chain and by improving the control system linearity. The redesign of the control system and detector amplifier chain and the addition of a mechanical viscous damper resulted in a three-fold increase in tracking range capability and significantly improved tracking stability and reliability.

B. SYSTEM DESCRIPTION

The optical platform is directly stabilized utilizing a 20 kilogram rotor at 3600 rpm, mounted in two axis gimbals which have a vertical axis and an axis perpendicular to the tracking beam. Torques to precess the gyro are applied by two-phase 60 Hz brushless ball bearing torque motors. Drum and wire couplings provide smooth, nearly frictionless torque with 12 to 1 mechanical advantage. One winding of each of the A.C. motors is provided with a fixed 60 Hz amplitude and phase. The second (quadrature) winding is provided with a 60 Hz signal at 90 degrees phase, with the amplitude being capable of varying through zero. The precession signals are generated by an analog computer so as to maintain the tracking optics, mounted on the gyro platform, pointed at the tracking beam source.

While the inherent stability of the gyro rotor removes a large portion of the ship's motion from the stable platform, error signals to the precession torque motors from the tracking analog computer are needed to maintain lock-on due to unwanted precession of the platform resulting from residual friction in the gimbal bearings. The control system also corrects for relative motion of the tracking beacon and the optical platform. The gyro optical system tracks an optical beacon chopped at a frequency of 1 kHz located onshore. The radiation from the beacon is collected using 60 mm optics as shown in Figure 1. This system produces a defocussed image

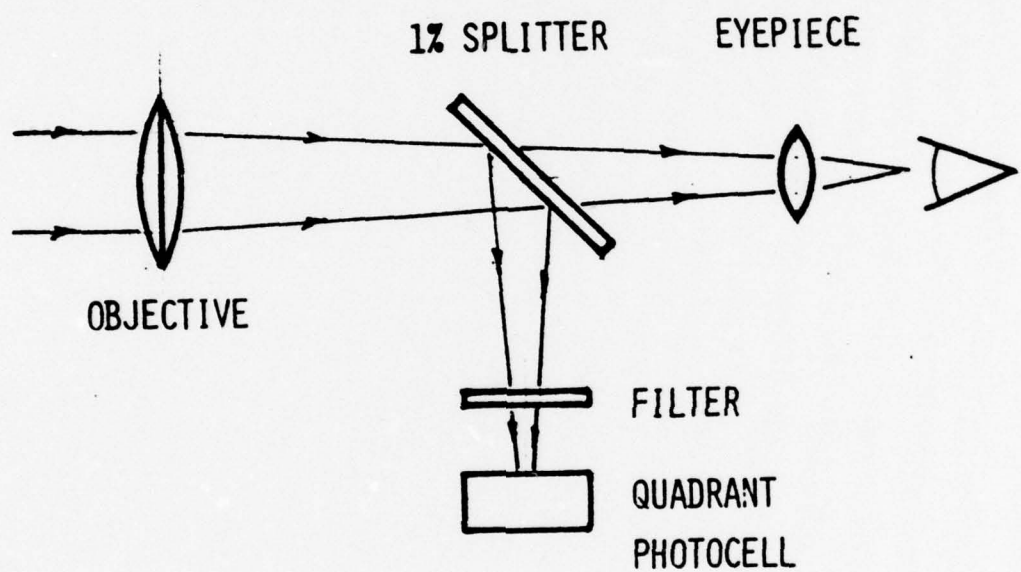


Figure 1
Diagram of Tracking Optics

on a quadrant photocell. An interference filter passing the tracking beacon wavelength is provided to reduce the background signal and unwanted signals from other chopped radiation sources near the beacon.

An analog tracking signal computer is utilized for control. A system block diagram is shown in Figure 2. Each quadrant photocell element signal is amplified, rectified and passed through a ripple filter to remove the chopping frequency components of the signal. After amplification and prior to rectification, the quadrant signals are also passed to a summing network and a sum signal from all quadrant signals is formed. This signal is then also rectified and passed through a ripple filter. The right-left difference signal and the up-down difference signal are then each divided by the sum signal to cancel scintillation effects. The scintillation-corrected right-left and up-down signals are utilized as proportional error signals to correct the gyro position. The up-down and right-left signals are also differentiated and added through a variable gain stage to the error signals for the quadrants at 90 degrees, to produce damping.

The output of the adders are power amplified and used to drive the two-phase torque motor power driver circuits. A joy-stick control provides a manual control capability for approach to lock-on.

The gyrostabilized platform and mounted optics are shown in Figure 3.

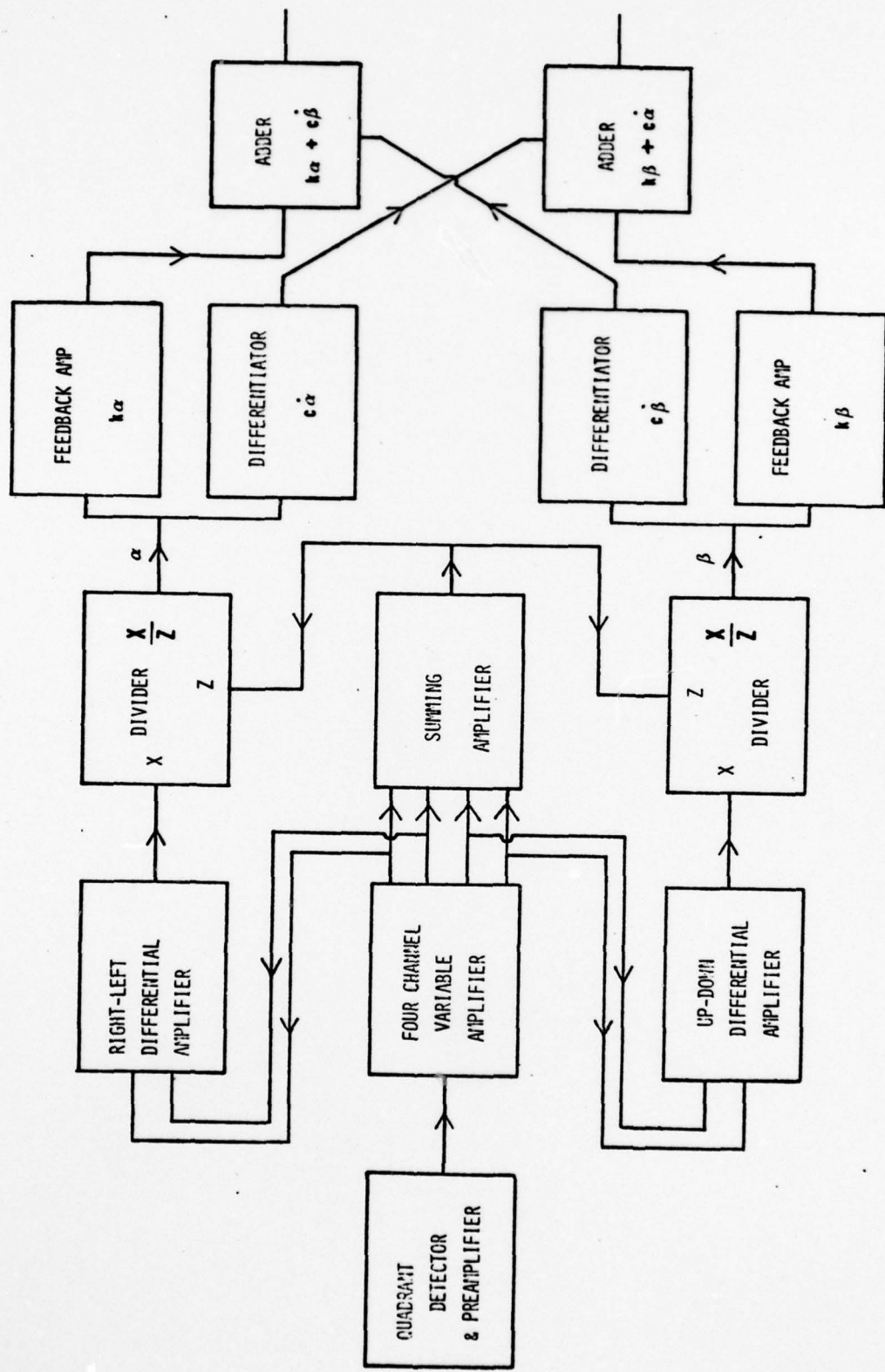
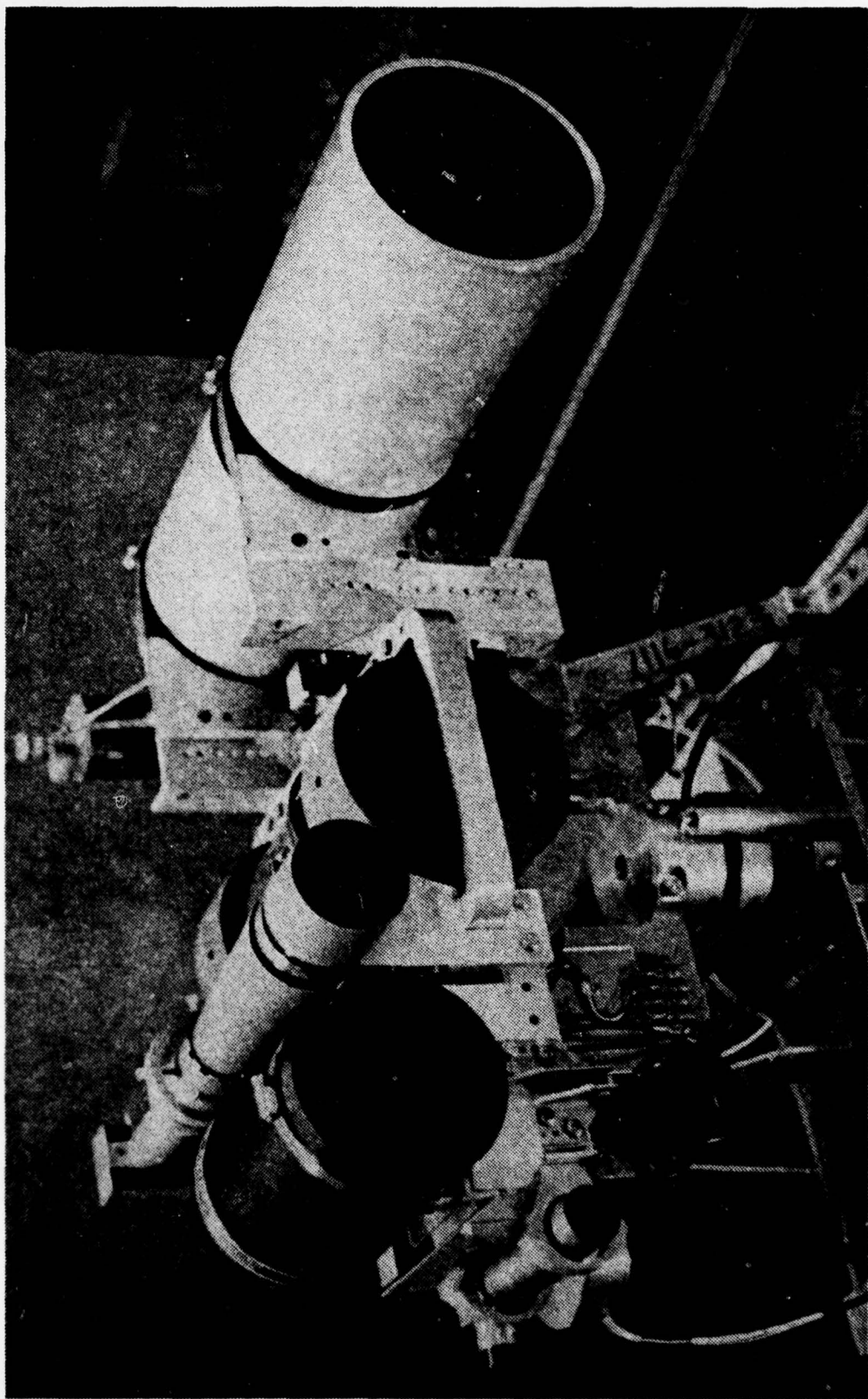


Figure 2
Control System Block Diagram

Figure 3
Gyro Stabilized Platform and Mounted Optics



II. CONTROL SYSTEM THEORY

A. STABILITY CRITERIA

The stabilized platform is a two-degree of freedom system. The system is free to rotate about the horizontal and vertical axes and is controlled so as to maintain the spin axis pointed at the tracking beacon. By analyzing the dynamics of a single axis the overall system dynamics can be understood.

Consider a system which can rotate about two axes \bar{X} and \bar{Y} as shown in Figure 4. Assume that \bar{X} , \bar{Y} and \bar{Z} define a fixed inertial reference frame. For this analysis it is assumed that O and L remain fixed with respect to the \bar{XYZ} reference frame and that B is free to pitch and yaw around O. This is a simpler motion than encountered in the actual operation of a shipboard gyro system but it is sufficient for understanding the system dynamics. Let the system gimbals S and G be supported in bearings so that they may be free to rotate about the pitch and yaw axes X and Y respectively. If the bearings were entirely frictionless, gimbals G and S would remain unaffected by the pitching and yawing motion of B. This is clearly an idealized situation which is not obtainable in practice. With friction present, any torque received due to the tendency of S to move about \bar{OY} will cause a precession about \bar{OX} . In addition, any torque received due to the tendency of G to move about \bar{OX} will cause a precession about \bar{OY} .

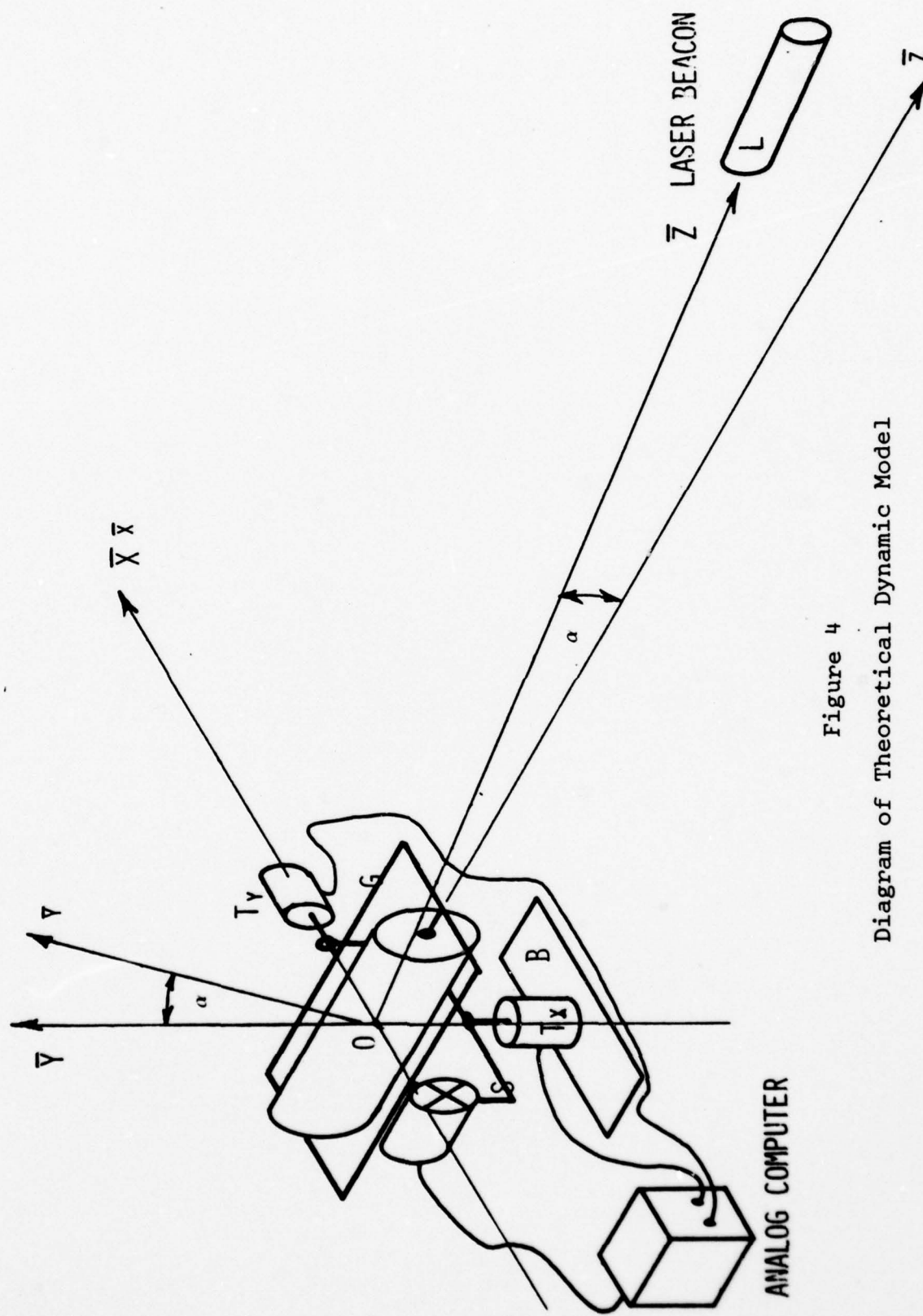


Figure 4
Diagram of Theoretical Dynamic Model

To maintain the $\bar{O}z$ axis directed at a specific point in space, as in the case with the shipboard gyro-stabilized optical platform, a quadrant detector and analog computer are introduced into the system to provide tracking signals to correct for motion of the ship relative to the tracking beacon and/or to correct errors due to the tendency of the system to precess due to frictional torques. The signals from the detector and computer, when power amplified, are passed to torque motors T_x and T_y to provide a compensating torque to S about $\bar{O}y$ and/or G about the $\bar{O}x$ axis.

To examine the dynamics of this system consider the effect of a small deflection α from the desired orientation of $\bar{O}z$ where θ denotes the absolute rotation about $\bar{O}y$ and α the rotation about $\bar{O}x$. The angular momentum of the gimbals and rotor about $\bar{O}y$ may then be written as

$$h_y = B''\dot{\theta} + (B+B')\dot{\theta}\cos^2\alpha - C(n-\dot{\theta}\sin\alpha)\sin\alpha + C'\dot{\theta}\sin^2\alpha \quad (1)$$

where B , B' and B'' denote the moments of inertia of the rotor about $\bar{O}y$, the gimbal G about $\bar{O}y$ and the gimbal S about $\bar{O}y$; C , C' those of the rotor and gimbal G about $\bar{O}z$ and n the constant angular velocity of the rotor relative to G . All moments of inertia other than B'' are assumed to be the principle moments.

Since we are considering $\bar{O}y$ as fixed, then assuming α small, the equation of motion about $\bar{O}y$ may be obtained from

Equation 1 as

$$T_m = h_Y = B_o \ddot{\theta} - Cn\dot{\alpha} \quad (2)$$

where $B_o = B + B' + B''$ and T_m is the torque supplied by the torque motor T_X . Taking A_o as the combined moment of inertia of rotor and gimbal G about \bar{Ox} , assuming a viscous damping torque $c\dot{\alpha}$ is applied by torque motor T_X and neglecting viscous friction of the gimbal bearings, the equation of motion about \bar{Ox} again assuming α small is

$$A_o \ddot{\alpha} + c\dot{\alpha} = -Cn\dot{\theta}. \quad (3)$$

The complete solution follows from Equations 2 and 3.

If the torque $T_m = k\alpha$ where k is a proportionality constant, the equations of motion become

$$k\alpha = B_o \ddot{\theta} - Cn\dot{\alpha} \quad (4a)$$

$$A_o \ddot{\alpha} + c\dot{\alpha} = -Cn\dot{\theta} \quad (4b)$$

from which

$$A_o \ddot{\alpha} + c\ddot{\alpha} + \frac{C^2 n^2}{B_o} + \frac{Cnk}{B_o} \alpha = 0. \quad (5)$$

Assuming that $\alpha = \alpha_0 e^{st}$ is a possible solution

$$A_0 s^3 + cs^2 + \frac{C^2 n^2}{B_0} s + \frac{Cn k}{B_0} = 0. \quad (6)$$

For stability the roots or real parts of the roots of Equation 6 must be negative and therefore α , the angular deviation goes to zero in time. This is satisfied if all the coefficients of s are positive and the product of the second and third coefficient is greater than that of the first and fourth. The first condition is obviously true and the second condition is

$$c > \frac{kA_0}{Cn}. \quad (7)$$

Equation 7 governs the overall system stability.

B. CLOSED LOOP FEEDBACK CONTROL

The gyro control system is a closed loop feedback system in which proportional error signals are generated to minimize detected angular deviations from optical alignment of the system with the tracking beacon. System feedback loops are illustrated in Figure 5. The normalized difference signals are proportional to the corresponding angular deviation in that direction. The derivative of the angular deviation analog signal is applied to the appropriate axis with appropriate polarity changes so as to create torques which viscously damp the system relative to the desired tracking direction.

The stability condition for the system as given in Equation 7 can be satisfied by adjusting k , the feedback loop gain and c , the damping coefficient.

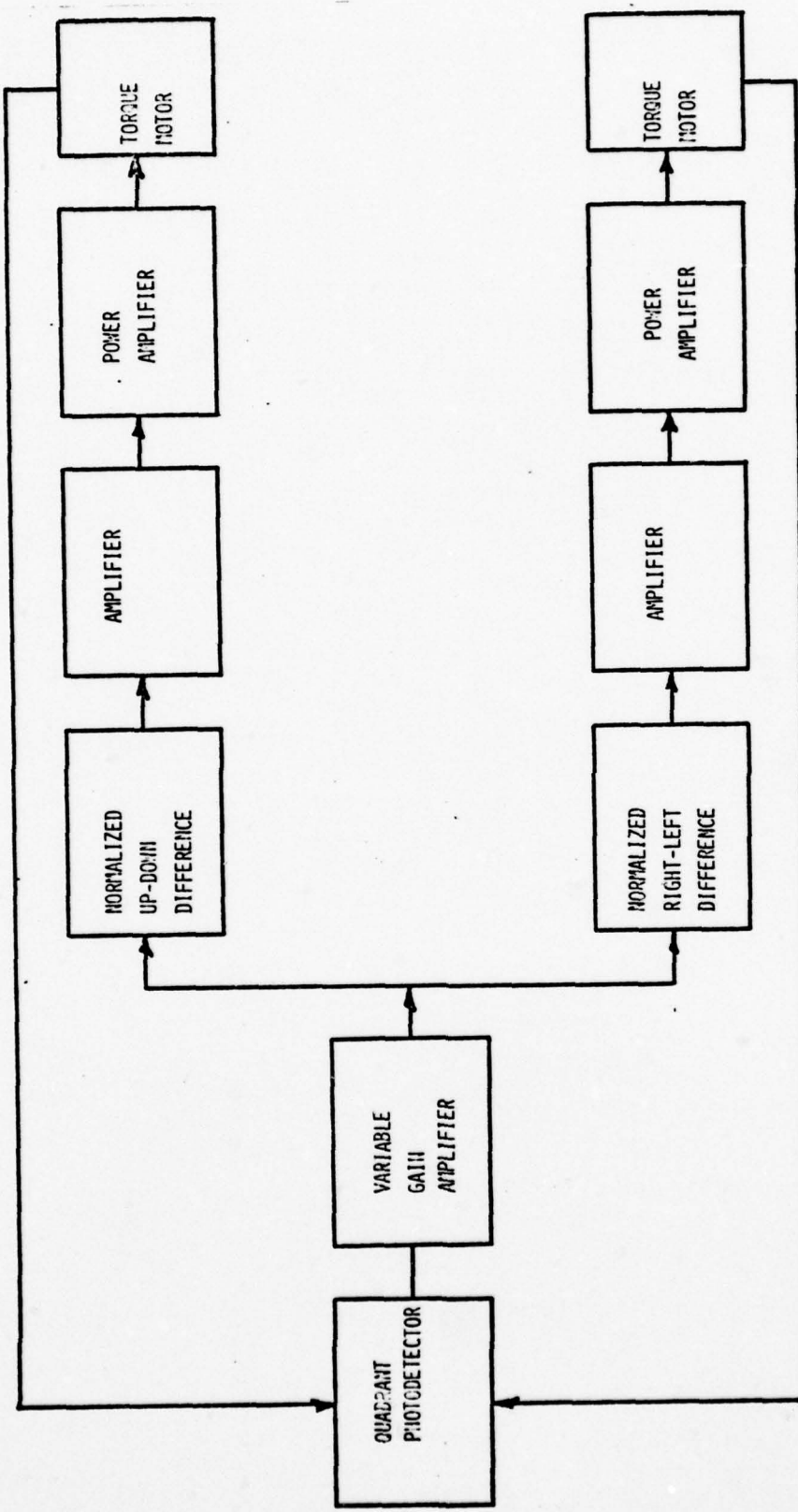


Figure 5
Diagram of Control System Feedback Loops

III. DETAILED CONTROL SYSTEM DESCRIPTION

A. DETECTOR

The optical signal from the tracking beacon is focused, using the tracker telescope optics, onto a PIN SPOT/4D United Detector Technology quadrant photodiode. This detector consists of four discrete elements and senses the ratio of the total amounts of light falling on the elements. Null and absolute position depend upon the light source being diffused on all elements. Therefore, the image on the photocell was defocused for increased signal linearity. The electrical characteristics of the detector is listed below.

Spectral response	3000Å-11000Å
Sensitivity (typical)	.4µa/µw
Response Time	<10 ⁻⁸ sec
N.E.P. (5 cps band width)	<10 ⁻¹² watts
Dark Current (each element @10v)	<5x10 ⁻⁷ amps
Capacity (each element)	2-15 pf
Element Separation	5 mils (.005 in)
R _c Effective Resistance between Elements	>1 meg ohm
Barrier Type	Diffused

Interference filters for .6328µm, 1.06µm and .4880µm can be interchanged so that a chopped source at any one of those wavelengths could be used as a tracking beacon. The system bandwidth will easily accomodate chopping frequencies in a range from 1-3 kHz.

B. DETECTOR PREAMPLIFIER

The output of each detector element is amplified using a high speed FET operational amplifier with a fixed gain of approximately 60. The outputs of the FET operational amplifiers are then A.C. coupled using a capacitor in series and transmitted from the detector head to the gyro control board using miniature coaxial cable. The detector and detector preamplifiers are contained within an enclosure attached to the tracking telescope shown in Figure 6. Circuit diagrams of all electronic circuits are contained in Appendix A.

C. VARIABLE GAIN AMPLIFIER

Because of a requirement for the system to operate over a wide range of input signal levels, a variable gain amplifier stage was developed so that the gain of the system could be raised to match the input signal level. This variable gain stage consists of two cascaded operational amplifiers, one stage with a gain varied by a trimming potentiometer and the second stage gain varied in steps by a front panel gain control knob. As the signal level from the output of the detector preamplifier varies, the gyro operator can adjust the gain on the front panel so that the signal level is within the linear operating region of the analog computer.

The A.C. coupled outputs of the FET operational amplifiers are fed into the variable amplifier stage. The system gain from the detector to the output of the variable amplifier stage can be adjusted in steps from 600 - 200,000. After

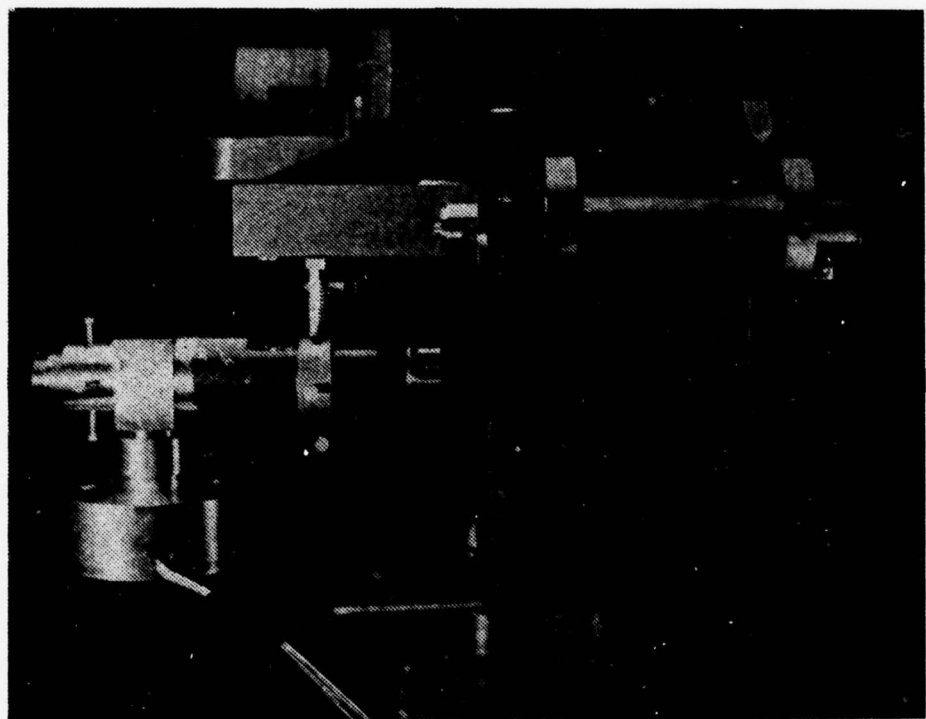


Figure 6
Tracking Telescope and Detector Head

amplification, the signals from all four detector elements are summed using an operational amplifier summing network. This summed signal is equivalent to the total signal level from the tracking beacon.

D. RECTIFIER AND RIPPLE FILTER

A.C. signals from each detector element and the summing network are rectified using a diode "clamping" circuit. The A.C. signal can be "clamped" to a D.C. level which can be adjusted positive or negative through ground. In actual operation, the signal was clamped to a slightly positive D.C. level. The rectified signals are then passed through an active ripple filter which approximately converts the 1 kHz square pulses to a D.C. level equal to the peak level of the pulses. In early performance tests, problems were encountered with phase shifts associated with this filter. The filter was modified so that no appreciable phase shifts would occur from 0 - 30 Hz. The gyro cannot react to frequencies higher than 10 Hz. Therefore, this solution virtually eliminated any phase related problems in the proportional error signal output.

E. ANALOG COMPUTER

The heart of the gyro control system consists of an analog computer which was designed to give proportional error signals to the precession torque motors so as to maintain a stable "lock-on" of the tracking optics to the tracking beacon.

Rectified and filtered signals from the elements of the quadrant photodiode are differenced in a pair of differential operational amplifiers. An analog error signal of appropriate sign results. The analog computer has two channels, one for up-down and one for right-left. The difference signals are then normalized by the sum signal in a divider circuit. The resulting signal is independent of the input signal level and as mentioned before, scintillation effects on the output of the computer are eliminated.

In addition to isolating the output error signal from scintillation effects, it was desirable that, with zero input signal level into the analog computer, the output error signals would also be zero. This would be the case when the tracking beacon is interrupted momentarily and therefore, both the difference and sum signals go to zero. Since the sum signal is the denominator input to the divider, without a non-zero input level the divider input would saturate since it would attempt to divide by zero. A simple solution to this problem would be to apply a D.C. bias to the sum signal. This solution, however, would result in a non-linear output from the divider. Therefore, a diode biasing arrangement was devised so that with a zero sum signal, a 1 volt bias was applied to the denominator input to the divider. As the sum signal level rose above 1 volt, the diode would become reversed biased and not conduct. As a result, the sum signal would again be unbiased, and the resulting divider output would be linear with sum signal levels above 1 volt.

From the divider the normalized signals are then sent to the final variable amplifying stage so that the overall error signal level could be varied to match the stability condition of the gyro system. This final variable amplifier has a front panel gain adjustment and this controls the gain of the gyro control feedback loops.

The sum signal level is a parameter which is convenient to monitor to maintain the input level of the computer within the normal operating range. The input level range for the computer is 1 volt D.C. minimum signal level and 10 volts D.C. maximum signal level. The input signal level is displayed on a meter on the gyro control panel.

Nutation is a problem encountered with almost any gyrodynamic system. Nutations of the gyrostabilized platform are damped using two systems, one electronic (within the analog computer) and a single axis mechanical viscous damper. The electronic damping is accomplished by taking the derivative of the divider output and adding the result with appropriate polarity inversions to the opposite axis error signals in an adder circuit. The differentiator output gains are variable so that stability criteria can be matched conveniently. A damping control knob is located on the main control panel. As a result, the electronic damping signal, which is superimposed on the error signal, drives the precession torque motors in such a way that they act like viscous dampers and oppose motion of the gyro platform relative to the desired directional orientation.

Power for the analog computer, detector and variable amplifiers is supplied by ± 15 volt 500 mA D.C. power supply.

F. MECHANICAL DAMPER

A mechanical viscous damper damps oscillations around the horizontal axis of the system. By damping oscillations around one axis of the system, the tendency for the system to nutate is greatly diminished. The damper consists of two conical discs separated by a thin film of fluid. Both discs rotate about the vertical axis of the system, one being directly coupled to the gyro motion and the other free to rotate independently. The latter is provided with relatively large moment of inertia by means of masses on two arms with adjustable radius for the masses. As the system rotates slowly, as is the case when tracking while the ship is turning, both discs rotate together coupled by the viscous effects of the fluid film and no torques are applied on the gyro system from the damper. If the gyro system attempts to oscillate, the discs begin to rotate relative to one another and damping torques are generated by the slippage of the discs. As a result, the oscillation is damped.

G. POWER AMPLIFIER

The outputs of the analog computer are power amplified using a current driver in conjunction with a matched Darlington power transistor pair. The power amplifier is supplied by a +15 volt 2 ampere D.C. power supply. The input to the

current drivers can be adjusted using a variable gain pre-amplifier if conditions require it. In actual practice, the power amplifier preamplifier gain was set at unity.

H. TWO-PHASE POWER DRIVER

The output of the power amplifiers are converted to an A.C. signal using a triac network. The output is an A.C. 60 cycle waveform of amplitude zero to about 120 volts (Figure 12).

I. JOY STICK CONTROL

Manual control of the system is accomplished using a "joy stick" input to the power amplifier. By manipulating the joy stick, D.C. voltage levels are applied to the up-down and right-left channels of the power amplifier so as to cause precession of the gyro platform. In this way the gyro system can be manually steered. This enables the system to be steered into "lock on" and in addition provides a secondary capability for course tracking in the event of computer failure in the field.

J. GYRO CONTROL PANEL

All operating controls are located on the gyro control panel as shown in Figure 7. The feedback loop gain control and damping control are located on the control panel as well as the variable gain signal amplifier control. An input signal level meter, right-left signal meter and up-down signal meter are also located on the panel. Attached below the panel is a

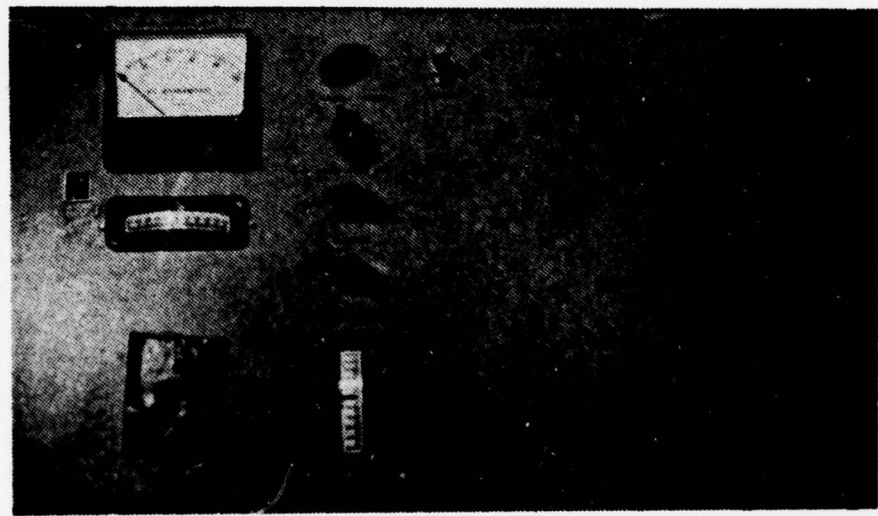


Figure 7
Gyro Control Panel

card rack for all control system electronics providing easy access for adjustment and troubleshooting. The electronics cards are shown in Figure 8.

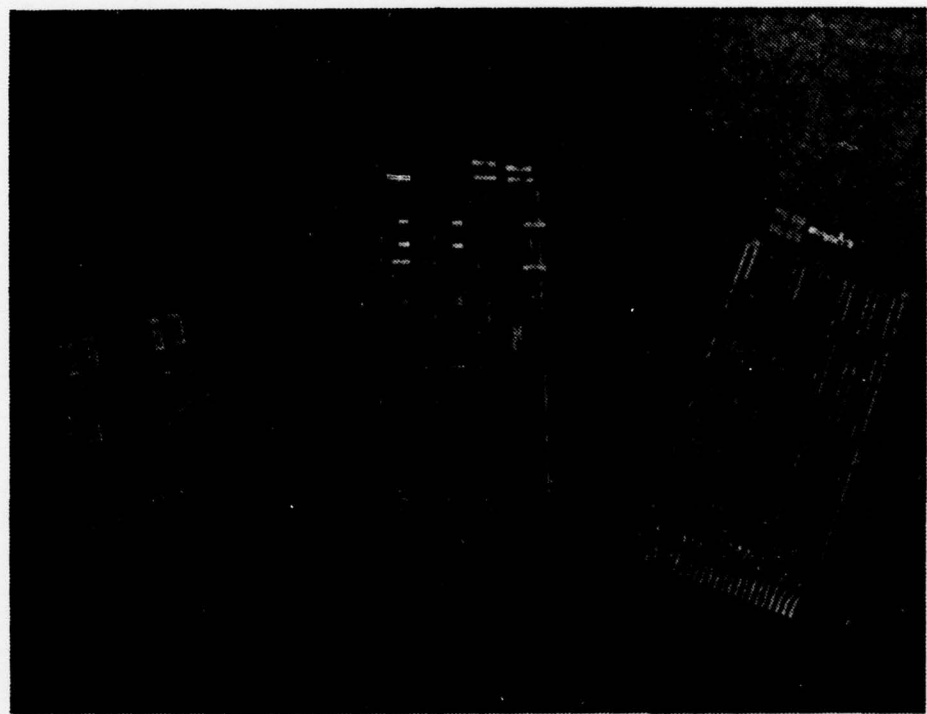


Figure 8
Control System Electronics Cards

IV. TEST RESULTS

Testing and evaluation of the gyro stabilized optical platform was divided into three separate test situations. Initial testing was conducted by positioning a $.6328 \mu\text{m}$ laser beacon at one end of a building corridor and placing the gyro system one hundred and thirty meters away at the opposite end of the corridor. Adjustment of the control system electronics was accomplished during this period. This test situation, while static, still provided insight into any obvious tracking problems. Neutral density filters were temporarily installed in the tracking optics to simulate a longer tracking range by attenuating the input optical signal. In addition, they prevented saturation of the variable gain amplifiers. Lock-on of the system was achieved out to a simulated range of 6.3 kilometers.

The second test situation consisted of placing a $.6328 \mu\text{m}$ laser tracking beam on the roof of Spanagel Hall, Building 232, Naval Postgraduate School, and the gyro system 2 kilometers away on the Research Vessel Acania moored to the Coast Guard pier in Monterey. This test was significant because the tracking range was characteristic of a normal operating range and the Research Vessel Acania, while moored to the pier, still provided a great deal of platform motion due to existing wind and sea conditions, so that tracking stability could be

tested. No significant problems were encountered and the system locked on with a tracking accuracy better than ± 2.5 milliradians (0.143°). A neutral density filter had to be placed in the tracker optics so that the signal level would not saturate the variable gain amplifiers at the minimum gain setting. The system was able to maintain lock-on for extended periods and lost lock only when the tracking beacon was interrupted for more than a second or when the platform was disturbed during work on the mounted optical systems.

The third test situation consisted of actual operation conditions during the CEWCOM-78 experiment conducted off of San Nicolas Island. A number of optical sources were located on shore and the gyro stabilized platform with optical receivers was mounted on the Research Vessel Acania anchored 2.3 kilometers offshore. Initial sea conditions were quite placid and the tracking system performed reliably and accurately, losing "lock-on" only when disturbed by work on mounted optical system or by more than momentary interruption of the tracking beacon. Tracking was accomplished using $.6328 \mu\text{m}$ and $.4880 \mu\text{m}$ lasers as tracking beacons.

Later during the experiment, the system was subjected to severe tracking conditions. The system was able to maintain a tracking accuracy of ± 2.5 milliradians during a strong gale with wind gusts of over fifty knots and state five seas (8-12 foot swells). The ship's motion was quite dramatic. The tracking system maintained lock-on until the ship's anchor chain parted and the experiment was aborted.

V. CONCLUSIONS AND RECOMMENDATIONS

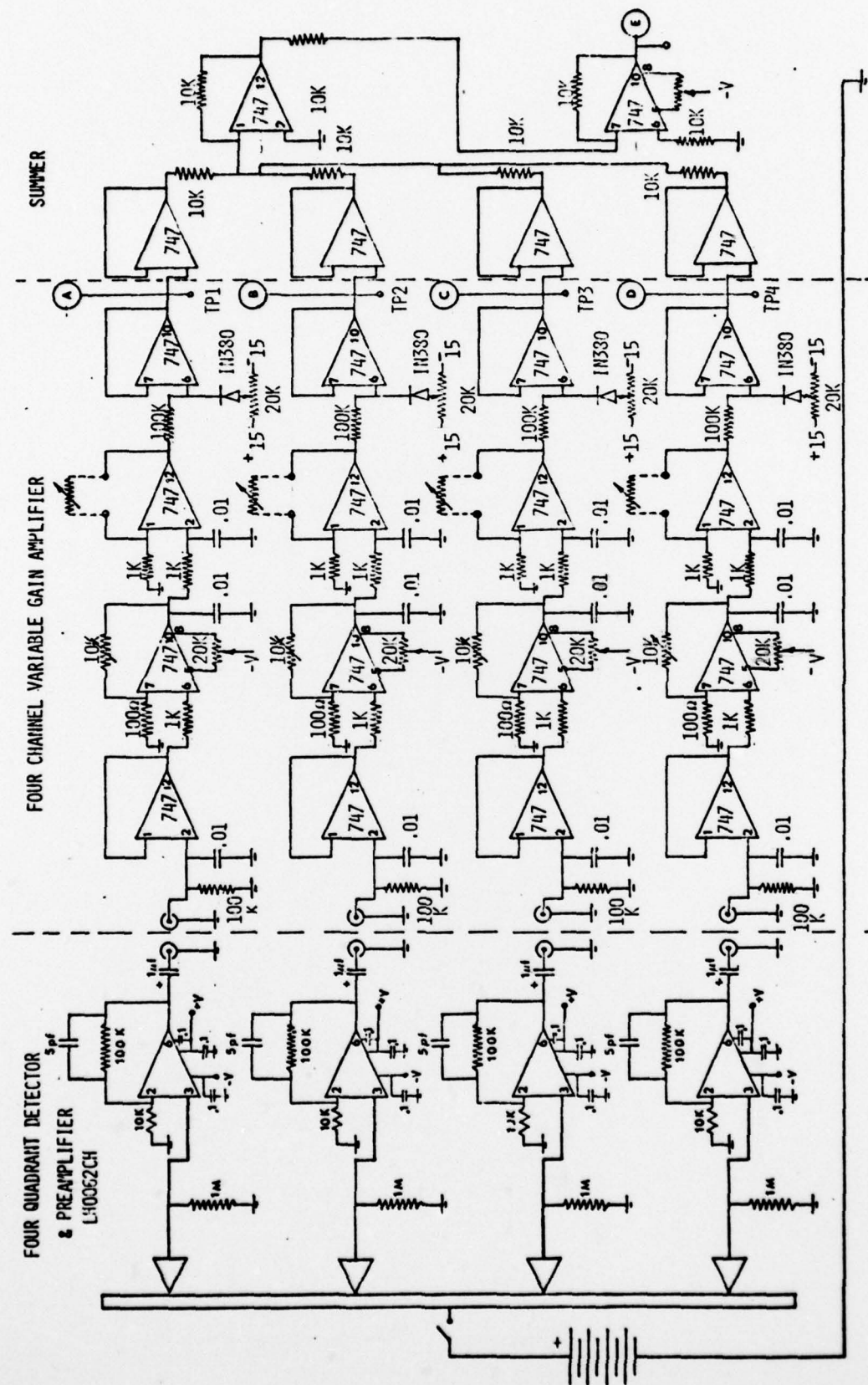
Performance of the shipboard gyro stabilized optical platform during CEWCOM-78 indicated that the system is capable of stable tracking with a tracking accuracy of better than ± 2.5 milliradians even under extremely adverse sea conditions.

The maximum range capability of the system was never actually approached in the field, however testing out to simulated range of 6.3 kilometers showed that lock-on could be achieved at that range. The system range capability could easily be increased by adding additional input signal gain stages to the control system and/or by increasing the size of the tracker optics.

The system could easily be adapted for slant path extinction measurements from ship to kytoon by either increasing the output capability of the two phase power driver circuit or by increasing the mechanical advantage of the torque motors. As a result, higher precession rates and thus faster tracking slew rates could be achieved. A second recommended modification of the system for kytoon tracking would be to increase the field of view of the tracking optics so that the acquisition field of view of the system would be increased.

APPENDIX A
Control Circuit Diagrams

Circuit diagrams for all control system electronics are shown in Figures 9 through 12.



Control Circuit Diagram, Section 1

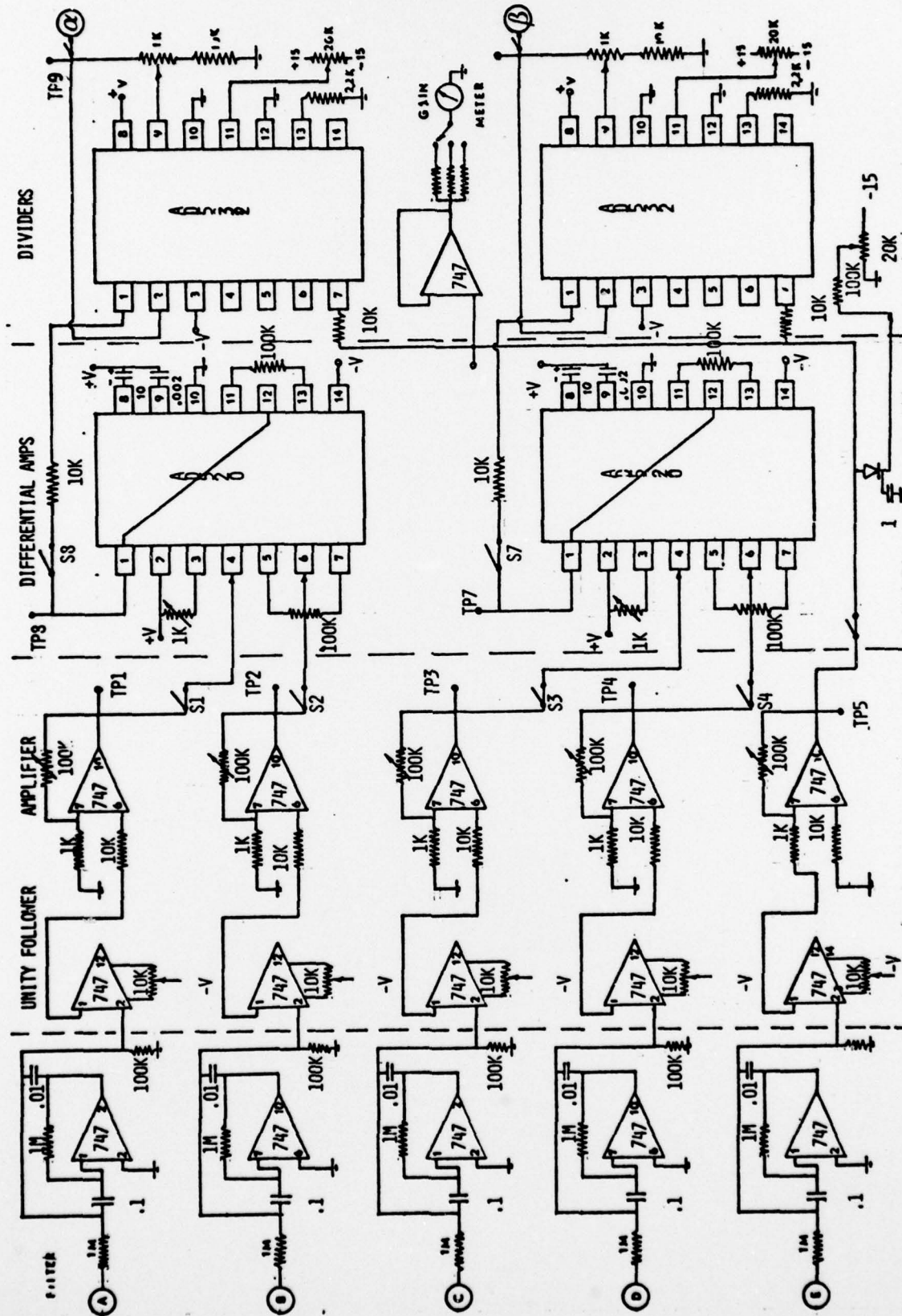
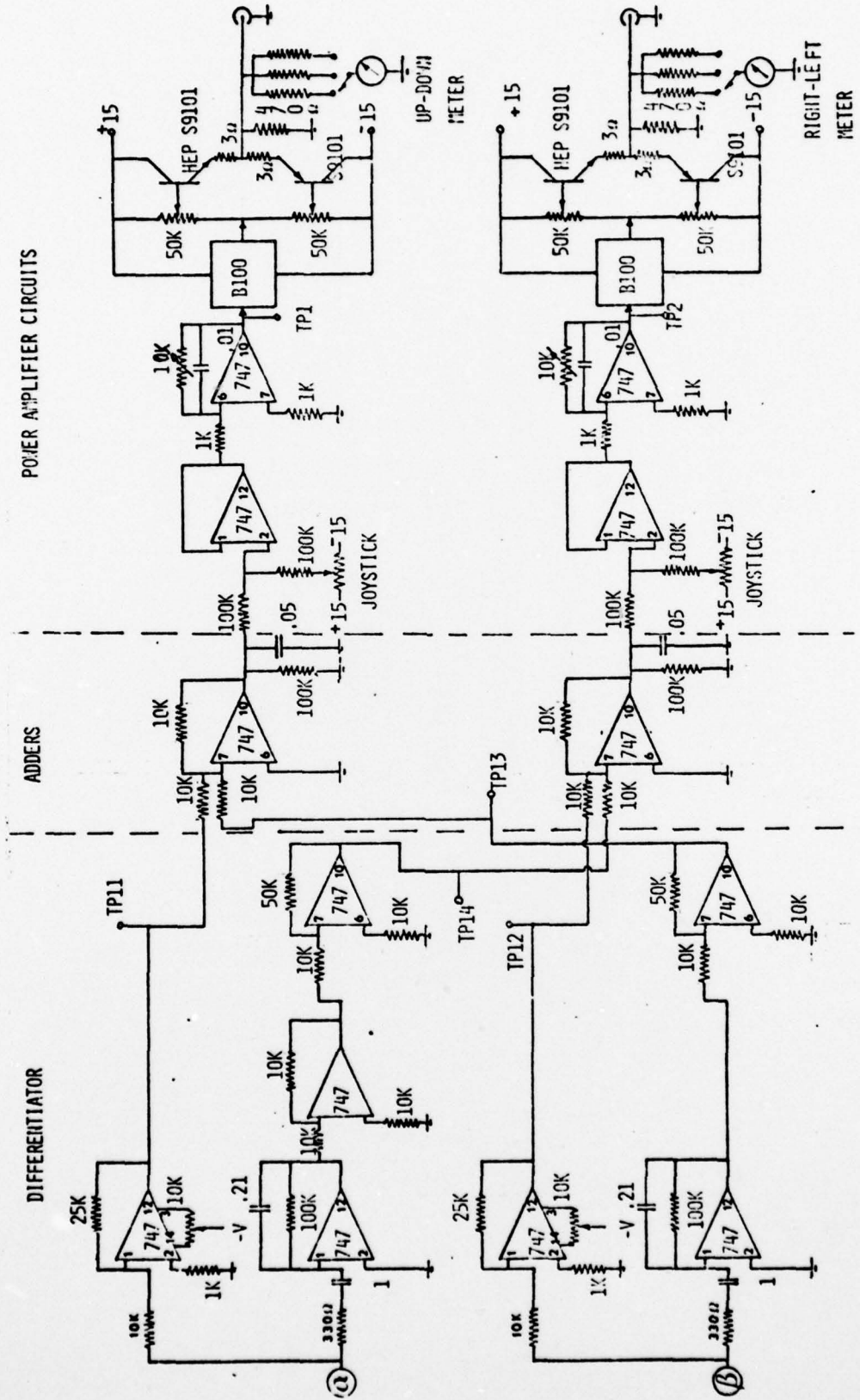


Figure 10

Control Circuit Diagram, Section 2



Control Circuit Diagram, Section 3

Figure 11

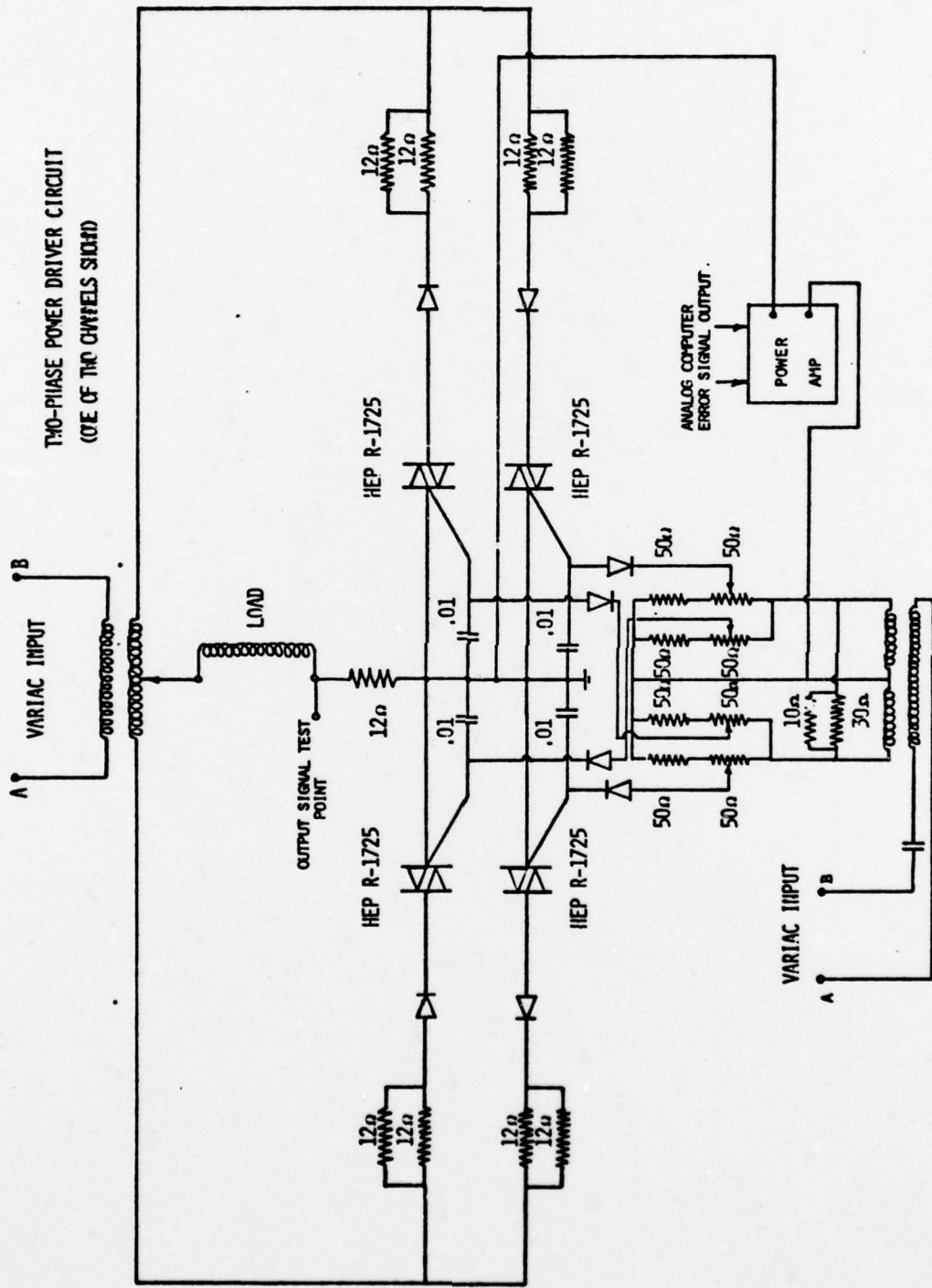


Figure 12
Two-Phase Power Driver Circuit Diagram

APPENDIX B

Control Circuit Adjustment Procedures

A. VARIABLE GAIN AMPLIFIER

1. Remove the detector head assembly.
2. Block out all light to the quadrant detector.
3. Turn on the power to the detector and gyro control panel. Allow the system to warm up for at least five minutes.
4. Adjust the offsets at test points one through five on the amplifier board to minimize any D.C. biases.
5. Defocus a chopped laser beam (preferably a .6328 μm He-Ne laser) onto the quadrant detector using the tracking telescope objective. Use neutral density filters to decrease the signal level to a non-saturating level.
6. Orient the detector so that all four elements are uniformly illuminated. Once this is accomplished, the signals out of the detector preamplifiers should be equal in amplitude at the four coaxial cable connections located on the card rack.
7. Adjust the four diode "clamping" trim potentiometers in conjunction with the amplifier offsets so that the signals are rectified.
8. Adjust the amplifier gain trim potentiometers so that the signal amplitudes at test points one through five are equal.

B. RIPPLE FILTER AND CONTROL BOARD

1. Adjust the variable gain amplifiers as previously described.
2. Block out all light to the quadrant detector.
3. Minimize the offsets at test points one through five on the control board. Adjust diode bias at test point six to -1 volt.
4. Uniformly illuminate the quadrant detector as previously described and adjust the gain of each filter amplifier so that the output signal levels are equal, with the exception of the sum signal filter, and are approximately equal to the value of the peak amplitude of the input signal to the filter. The input and output levels of the sum signal filter should be four times that of the other channels.
5. Adjust the offset of the differential amplifiers and the dividers so that their outputs are zero with the detector uniformly illuminated.
6. With the damping control on the gyro control panel turned completely counter-clockwise, turn the stiffness control approximately half way on. Check the offset of the dividers at test points eleven and twelve and adjust the divider offsets again if necessary.

LIST OF REFERENCES

1. Arnold, R.N. and Maunder, L., Gyrodynamics and its Engineering Applications, Academic Press, 1961.
2. Denhard, W.G., Hollister, W.M. and Wrigley, W., Gyroscope Theory, Design and Instrumentation, M.I.T. Press, 1969.
3. Machover, C., Basics of Gyroscopes, V. 2, John F. Rider Publisher, 1960.

INITIAL DISTRIBUTION LIST

	No. Copies
1. Defense Documentation Center Cameron Station Alexandria VA 22314	2
2. Library, Code 0142 Naval Postgraduate School Monterey CA 93940	2
3. Department Chairman, Code 61 Department of Physics and Chemistry Naval Postgraduate School Monterey CA 93940	2
4. Professor E.C. Crittenden, Jr., Code 61Ct Department of Physics and Chemistry Naval Postgraduate School Monterey CA 93940	3
5. Professor G.W. Rodeback, Code 61Pk Department of Physics and Chemistry Naval Postgraduate School Monterey CA 93940	1
6. Robert C. Smith, Code 12A Research Administration Naval Postgraduate School Monterey CA 93940	1
7. LT R.L. Williams 13233 Clifton Road Silver Spring MD 20904	1